

The Design of Finite-time Convergence Guidance Law for Head Pursuit based on Adaptive Sliding Mode Control

Cheng Zhang^{1,2}, Ke Zhang^{1,2} and Jingyu Wang^{1,2}

¹*School of Astronautics, Northwestern Polytechnical University, Xi'an 710072, China*

²*National Key Laboratory of Aerospace Flight Dynamics, Northwestern Polytechnical University, Xi'an 710072, China*

Keywords: Finite-time Convergence, Head Pursuit, Terminal Sliding Mode, Sliding Mode Control.

Abstract: The high-speed target interception plays a vital role in the modern industry with many application scenarios. Due to the difficulties of direct interception in high speed, the head pursuit intercept is frequently considered for the target of re-entering flight vehicle. In this paper, a novel terminal sliding mode control method is proposed for the interception of high-speed maneuvering target, in which the finite convergence guidance law is initially designed under the constraint of intercept angle. By introducing the mathematical model of correlative motion between interceptor and target, the sliding surface is researched and designed to meet the critical conditions of head pursuit intercepting. Meanwhile, considering the dynamic characteristics of both interceptor and target, an adaptive guidance law is therefore proposed to compensate the modelling errors, which goal is to improve the accuracy of interception. The stability analysis is theoretically proved in terms of the Lyapunov method. Numerical simulations are presented to validate the robustness and effectiveness of the proposed guidance law, by which good intercepting performance can be supported.

1 INTRODUCTION

In recent years, high-speed targets such as re-entering flight vehicle have brought severe challenges to the traditional interception system. Hypersonic vehicle target requires higher accuracy of the interception system, such as long distance target detection, the quick response of each subsystem in the system, the ability to withstand high temperature of seeker and the ability of the guidance system to adapt to harsh aerodynamic environment interference and so on.

Generally speaking, the requirement for the speed of interceptor is higher than the target in the terminal interception process, it is therefore not very suitable for the traditional rear-end interception issue. However, considering the head-on interception, due to the extreme high speed of the target, it will cause the missile - target relative speed become very large. Therefore, it will cause more stringent requirements to the computation capacity of the computer as well as other hardware devices on-board. Since all these requirements cannot be achieved in a very short time, the designing of appropriate control method will be a practically realizable way.

To solve the problem of interception in the high

speed situation, the head pursuit(HP) interception is proposed (Shima, 2007). By using the HP interception, not only the seeker can be protected from the vital influence of high temperature and bad aerodynamic interference, but also the energy consumption of the interceptor can be reduced. Therefore, the research of HP interception has attracted huge attention in recent years.

As a frequently used design method in control system, the flexibility of sliding mode control (SMC) is strong. As the dynamic characteristic of a control system is related to the designed sliding surface, so when the control system is running on a specifically designed sliding surface, the quality of which will significantly affect the performance of the system.

In fact, as long as the system is assured to finally approach the sliding surface and satisfy the stability condition, there will be no limit to the form of used sliding surface. Therefore, how to design a sliding surface with better control performance has become the focus of research, from which also derived a lot of new SMC methods (Goyal, 2015). However, traditional SMC approaches generally use the linear sliding surface, thus the system is only asymptotic convergence in this case. If the target is with complex non-linearity property, good control

performance cannot be achieved by applying the traditional method or even worse, the stability of system cannot be guaranteed. However, a terminal sliding mode (TSM) control method that can converge to zero in finite time is initially proposed in (Zhihong, 1994), which has opened up a new research field of SMC. Thereafter, the TSM based control method has become one of the hot topics in the research of SMC (Feng, 2013 and Kumar, 2014).

2 RELATED WORKS

In the research of sliding mode control method, the essential key is to design the guidance law. Due to the fact that relative motion equations of target and interceptor have strong nonlinear cross coupling, parameter uncertainty and external disturbance inevitably exist, so the target interception system is a nonlinear uncertain system.

To deal with the control issue of this complex system, many research methods have been proposed in recent years. In the research works of (Liu, 2010 and Li, 2011), two control methods are presented to solve the control problem of the classic SISO and MIMO nonlinear system, in which the variable structure control and fuzzy control theory are used respectively. Though the achieved results have shown that good outputs can be obtained by applying the proposed methods, the target systems that considered in these works are simple.

Regarding the control problem of the complex system in real world, a fuzzy terminal sliding mode control strategy is proposed in (Gu, 2015) for the control of marine current power system. The proposed control strategy mainly consists of two major parts, which are a fuzzy logic controller for deriving the reference generator current and a non-singular terminal sliding mode controller to track the aforementioned derived current, respectively. Meanwhile, in the work of (Zhao, 2015), an output feedback terminal sliding mode control framework for the continuous stirred tank reactor is presented. In this work, two novel control algorithms of TSM are studied, of which the theoretical stability analysis is given. The experimental results of above-mentioned works show that, if appropriate designed, the TSM based control approaches can be effective solutions to deal with the nonlinear system, while its robustness to external disturbance is superior to the traditional research works. However, the high-speed target is a highly nonlinear system which far more complex than the system considered in the industrial application scenario. Therefore, the presented works

have obvious limitations and thus cannot be applied on the interception, which bring out the requirement of novel control method.

In the work of (Behera, 2015), the steady-state behaviour of discretized TSM control is comprehensively studied, in which the continuous-time system is discretized and the analysis of steady-state behaviour is given in the terms of periodic orbits. By finding all possible orbits, the research reveals that only period-2 orbit is satisfied by the state evolution and thus retained in steady-state. Though the analytic result is achieved by only considering a second-order system, it can be developed for a n th order SISO system as well. This work shows that the continuous-time system can be theoretically researched by conducting a discretized processing, which supports promising application in the design of TSM control method for higher order nonlinear complex system. Moreover, a non-singular TSM controller is proposed for actuated exoskeleton in (Madani, 2015), of which the target system is actually an active orthosis used for rehabilitation purpose. Since the system has a complex dynamical model with no prior knowledge, the proposed controller uses non-singular TSM technique to obtain the expected good performance in terms of convergence in a finite time. Supported by the theoretical stability proof in closed loop, the proposed approach is ensured to be stable according to the Lyapunov formalism. Experimental results have shown that smooth movements could be conducted for flexion and extension, which indicates the potential application in real world. However, it should be pointed out that, the system considered in this work is still not as complex as the target system considered in the interception scenario, which shows that improvement of previous proposed approaches should be researched.

Considering the specific control target system of spacecraft, a SMC approach is designed in (Lu, 2012), in which the existence of external disturbances and inertia uncertainties are both taken into account. The simulation results show that, the proposed approach is capable to achieve the goal of effectively tracking on the attitude of a spacecraft. Meanwhile, a novel adaptive sliding mode control scheme for spacecraft body-fixed hovering in the proximity of an asteroid is proposed in (Lee, 2015). Since the bounds of parametric uncertainties as well as the disturbances are not required in advance, the scheme is proposed to guarantee the asymptotic stability of states for both position and attitude stabilization. The achieved results of numerical simulation have demonstrated both low control

inputs and effectiveness of control strategy. Though both of these works have shown that sliding mode control method is a practically useful tool for the control issue of spacecraft, the targets considered in these systems are regular spacecraft with normal speed, which cause the limitations when apply them on the HP interception problem.

Particularly, a HP sliding mode variable structure guidance law is introduced in the work of (Hua, 2011), in which the deviation and related derivative are used as switching function by using the Lyapunov method. Although it can obtain better results for the case of high-speed interception, much more information of the system is required, which is difficult to achieve. The research work accomplished in (Song, 2015) is similar to our work, in which the design of a guidance law for non-decoupling 3D engagement geometry is studied. By using finite time integral sliding mode manifold, an improved control law is developed to estimate the upper bound of the target acceleration. Experiment results show that, the proposed control method can control the target in both constant speed and varying speed situations effectively. However, despite that the target can be precisely intercepted by applying the proposed method, the designed control laws are specifically developed regarding the classic way of interception which is different from HP interception.

Consequently, novel control method for the HP interception system should be theoretically studied. In this paper, by considering the target maneuvering as bounded uncertain item of the system, an adaptive sliding mode guidance law suitable for head pursuit interception scenario is proposed. The derivation of the designed guidance law is based on the dynamic characteristics of both interceptor and target, while their model errors are taken into account as well. The stability analysis of the proposed TSM adaptive control method is studied by providing the detailed theoretical proof. Finally, simulation experiments show that robustness and convergence in finite time could be achieved for the HP interception.

3 OVERVIEW OF HEAD PURSUIT INTERCEPTION

3.1 HP Working Process

The schematic diagram is shown in Figure 1. In general, the head pursuit intercept can be divided into three phases: a) approach; b) control the orbit direction of interceptor to enter the preset orbit at a

predetermined time; c) terminal guidance.

The major task of interception in the terminal process is to adjust the position as well as direction of the interceptor flight errors, while making the tail of interceptor as close as to the target, then intercept the target head.

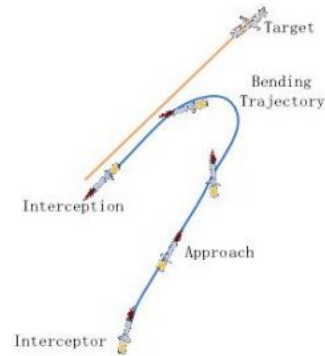


Figure 1: Head pursuit interception.

3.2 HP Kinematic Equation

In the stage of the terminal guidance, the interceptor will fly in the same general direction as the target, while ahead of it at a lower speed. Because of the relatively short interception time and the overload restriction, the interceptor flight direction will rarely change. As a result, the interception process can be decoupled into two orthogonal planes, which are vertical plane and horizontal plane respectively. Correspondingly, the expected guidance law can be designed in the two planes.

To simplify the problem of HP interception, we assume that the interceptor and the target can be treated as a particle. The acceleration vectors of both interceptor and target are vertical with their velocity vector, thus the acceleration vector will only change the velocity of the interceptor and target, while the direction will not change.

Considering the case in the longitudinal plane as an example, the planar geometry is shown in Figure 2. It can be seen that, the target T is located behind the interceptor I which has lower speed. Here, the speed, maneuvering acceleration and flight-path angle are respectively denoted by V , a and γ . The range between the target and interceptor is defined as r , while q is the line of sight (LOS) angle relative to a fixed reference. Meanwhile, the angles θ and δ are the instantaneous target and interceptor direction of flight relative to the LOS.

In Figure 2, the V_r denotes the relative speed between the interceptor and target, which is defined as

$$V_r = V_I \cos \delta - V_T \cos \theta \quad (1)$$

and the speed perpendicular to the LOS is

$$V_q = V_I \sin \delta - V_T \sin \theta \quad (2)$$

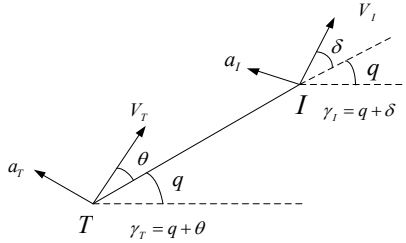


Figure 2: HP geometry.

Therefore, we can have the equations of HP interception as follows

$$\begin{cases} \dot{r} = V_r = V_I \cos \delta - V_T \cos \theta \\ \dot{\theta} = a_T / V_T - V_q / r \\ \dot{\delta} = a_I / V_I - V_q / r \\ \dot{q} = V_q / r \end{cases} \quad (3)$$

Meanwhile, the speeds of interceptor and target are represented by V_I and V_T , respectively. Thus, the speeds should be constant and non-dimensional parameter K can be defined as the speed ratio as

$$K = V_I / V_T < 1 \quad (4)$$

Let the running time is t , the terminal guidance initials at $t = 0$ with $\dot{r}(t = 0) < 0$ and terminates at $t = t_f$ where

$$t_f = \arg \{ r(t) \dot{r}(t) = 0 \} \quad (5)$$

Considering the goal of successfully intercept, the conditions that must be met are as follow

$$\lim_{t \rightarrow t_f} r(t) = 0 \quad (6)$$

$$\begin{cases} \lim_{t \rightarrow t_f} \theta = 0 \\ \lim_{t \rightarrow t_f} \delta = 0 \end{cases} \quad (7)$$

The purpose of HP guidance control is to guide the interceptor to the point that satisfies the conditions of Eq.(6) and Eq.(7). Therefore, the angles θ and δ need to be proportionally changed during the design process

$$\delta = n\theta \quad (8)$$

where n is guidance coefficient.

Nevertheless, in the real interception scenario, the interceptor might need to hit the target with a

certain angle which brings more requirements to the designed control law. Therefore, it is quite necessary to put forward a more objective terminal interception geometric condition, thus the Eq. (8) is amended as

$$\delta - \delta_r = n(\theta - \theta_r) \quad (9)$$

where $|\theta_r| < \pi/2$ is selected purposely and

$$\delta_r = \sin^{-1} [\sin(\theta_r) / K] \quad (10)$$

4 PROPOSED APPROACH

At the very beginning of the design of guidance law, we should determine the dynamic of the interceptor and target, and then we use the TSM control to design the guidance law, finally prove the stability.

In order to compensate the interference of both model errors and external disturbances, the finite time convergence adaptive reaching law is designed, the design method is based on the following three steps: First, select the proper sliding surface. Second, design the adaptive guidance law. Finally, prove the stability of both processes in either reaching phase or in sliding phase.

4.1 Dynamic

Though Eq.(9) describes the geometric rule between the interceptor and target, the explicit control value is however not included. Therefore, it is necessary to derive relationship between this rule and interceptor acceleration command a_I .

We assume that closed-loop lateral acceleration of both interceptor and target can be represented by equivalent first-order transfer function, by ignoring model error we have

$$\dot{a}_I = (a_{Ic} - a_I) / \tau_I \quad (11)$$

$$\dot{a}_T = (a_{Tc} - a_T) / \tau_T \quad (12)$$

where a_{Tc} , a_{Ic} are the guidance commands of target and interceptor, τ_T and τ_I are their time constants. Notably, the acceleration command is restricted to

$$|a_T^c| \leq M_{T \max} \quad (13)$$

4.2 Sliding Surface Design

In contrast to the existing methods of HP intercept guidance law, this paper uses the terminal sliding mode surface which can converge in a finite time.

We define the HP interception deviation as

$$e = \delta - \delta_r - n(\theta - \theta_r) \quad (14)$$

where n is the time constant. Since interceptor and target have first order characteristics, the derivation of e is required to have the accelerate command a_{lc} .

Lemma 1. (Yu, 2005) For any real numbers $\lambda_1 > 0$, $\lambda_2 > 0$, $0 < k < 1$, an extended Lyapunov condition of finite-time stability can be given in the form of TSM as

$$\dot{V}(x) + \lambda_1 V(x) + \lambda_2 V^k(x) \leq 0 \quad (15)$$

where the settling time can be estimated by

$$T_r \leq \frac{1}{\lambda_1(1-k)} \ln \frac{\lambda_1 V^{1-k}(x_0) + \lambda_2}{\lambda_2} \quad (16)$$

Define the terminal sliding variable as

$$s = \dot{e} + \beta |e|^\alpha \text{sign}(e) \quad (17)$$

where $\beta > 0$, $0 < \alpha < 1$. Substituting Eqs (1), (2), (3), and (14), we can write the sliding variable as

$$\begin{aligned} s &= \dot{\delta} - \dot{\delta}_r - n\dot{\theta} + n\dot{\theta}_r + \beta |P| \text{sign}(P) \\ &= \frac{a_I}{V_I} - n \frac{a_T}{V_T} + (n-1) \frac{V_\lambda}{r} + \beta |P| \text{sign}(P) \end{aligned} \quad (18)$$

where $P = \dot{e}$, and differentiating the Eq. (18) as

$$\begin{aligned} \dot{s} &= \frac{a_{lc} - a_I}{\tau_I V_I} - n \frac{a_{Tc} - a_T}{\tau_T V_T} + (n-1) \frac{a_I \cos \sigma - a_T \cos \theta}{r} \\ &\quad - (n-1) \frac{2V_\lambda}{r} \dot{q} + \beta \alpha |e|^{\alpha-1} \left[\frac{a_I}{V_I} - n \frac{a_T}{V_T} + (n-1) \dot{q} \right] \end{aligned} \quad (19)$$

Substituting Eqs.(1), (2) and (3), into Eq.(19) as

$$\dot{s} = G_I a_I + G_T a_T + G_\lambda \dot{q} + G_{lc} a_{lc} + G_{Tc} a_{Tc} \quad (20)$$

where

$$\begin{cases} G_I = -\frac{1}{\tau_I V_I} + (n-1) \frac{\cos \delta}{r} + \beta \alpha |e|^{\alpha-1} / V_I \\ G_T = \frac{n}{\tau_T V_T} - (n-1) \frac{\cos \theta}{r} - n \beta \alpha |e|^{\alpha-1} / V_T \\ G_\lambda = -2(n-1) \frac{V_\lambda}{r} + (n-1) \beta \alpha |e|^{\alpha-1} \\ G_{lc} = \frac{1}{\tau_I V_I} \\ G_{Tc} = -\frac{n}{\tau_T V_T} \end{cases} \quad (21)$$

Therefore, the first-order dynamic characteristic of sliding variable can be simplified to

$$\dot{s} = G_I a_I + G_T a_T + G_q \dot{q} + G_{lc} a_{lc} + G_{Tc} a_{Tc} \quad (22)$$

4.3 Guidance Law Design

Based on the terminal sliding variable given in Eq.(17), the sliding mode controller a_{lc} can be composed of two parts: a_{eq} and a_{uc} .

To be specific, a_{eq} is called the equivalent part, which indicates that if there is no model error and target maneuvering, the system could continue to approach within the sliding surface. Meanwhile, a_{uc} is called the uncertainty part, which means that if the system has modelling errors and target maneuvering, this part can drive the system to the designed sliding surface s , so that the robustness of the system can be achieved. Therefore, a_{lc} can be written as

$$a_{lc} = a_{eq} + a_{uc} \quad (23)$$

$$a_{eq}(t) = -(G_I a_I + G_T a_T + G_\lambda \dot{q}) / G_{lc} \quad (24)$$

In this paper, we design the uncertainty part of a_{uc} based on the reaching law as

$$\dot{s}_k = -k_1 s - k_2 \text{sig}^\rho(s) \quad (25)$$

where $k_1 > 0$, $k_2 > 0$, $0 < \rho < 1$. According to Eq. (22) and Eq.(25), it can be written as

$$a_{uc}(t) = \begin{cases} -(\hat{k}_1 s + \hat{k}_2 \text{sig}^\rho(s)) / f_{lc} & \|s\| \geq \varepsilon \\ 0 & \|s\| < \varepsilon \end{cases} \quad (26)$$

where \hat{k}_1, \hat{k}_2 are the estimated gain values. For the research objective in this paper, it is better to eliminate the influence of external disturbance and accelerate the convergence speed of the sliding surface, thus the adaptive law can be designed as

$$\dot{\hat{k}}_1 = \begin{cases} \eta_1 \|s\|^2 & \|s\| \geq \varepsilon \\ 0 & \|s\| < \varepsilon \end{cases} \quad (27)$$

$$\dot{\hat{k}}_2 = \begin{cases} \eta_2 \|s\|^{\rho+1} & \|s\| \geq \varepsilon \\ 0 & \|s\| < \varepsilon \end{cases} \quad (28)$$

where $\eta_1, \eta_2, \varepsilon$ are positive design parameters.

4.4 Stability Proof

Proof. We select the Lyapunov function as

$$V = \frac{1}{2} s^T s + \frac{1}{2\eta_1} k_1^{-2} + \frac{1}{2\eta_2} k_2^{-2} \quad (29)$$

By using the time derivative of the Lyapunov function, we have

$$\begin{aligned}
 \dot{V} &= s^T \left(-\hat{k}_1 s - \hat{k}_2 \text{sig}^\rho(s) + G_{Tc} a_{Tc} \right) \\
 &+ \left(\hat{k}_1 - k_1 \right) \|s\|^2 + \left(\hat{k}_2 - k_2 \right) \|s\|^{\rho+1} \\
 &\leq -\hat{k}_1 s^2 - \hat{k}_2 \|s\|^{\rho+1} + \left(\hat{k}_1 - k_1 \right) \|s\|^2 \\
 &+ \left(\hat{k}_2 - k_2 \right) \|s\|^{\rho+1} + |G_{Tc} a_{T \max}| \|s\| \\
 &\leq -k_1 \|s\|^2 - k_2 \|s\|^{\rho+1} + |G_{Tc} a_{T \max}| \|s\|
 \end{aligned} \quad (30)$$

In order to make $\dot{V} < 0$, Eq.(30) can be rewritten into the following two forms as

$$\dot{V} \leq -2 \left(k_1 - \frac{G_{Tc} a_{T \max}}{\|s\|} \right) V - 2^{\frac{\rho+1}{2}} k_2 V^{\frac{\rho+1}{2}} \quad (31)$$

$$\dot{V} \leq -\frac{k_1}{2} V - 2^{\frac{\rho+1}{2}} \left(k_2 - \frac{G_{Tc} a_{T \max}}{\|s\|^\rho} \right) V^{\frac{\rho+1}{2}} \quad (32)$$

If we want to make $\dot{V} < 0$, the initial values of parameters k_1 and k_2 should meet the following conditions as

$$k_1 > \frac{|G_{Tc} a_{T \max}|}{\|s\|} \quad (33)$$

$$k_2 > \frac{|G_{Tc} a_{T \max}|}{\|s\|^\rho} \quad (34)$$

Consequently, both Eq.(31) and Eq.(32) can be simplified as

$$\dot{V} + \lambda_1 V + \lambda_2 V^{\frac{\rho+1}{2}} \leq 0 \quad (35)$$

where $\lambda_1 = -k_1/2$, $\lambda_2 = 2^{\frac{\rho+1}{2}} k_2$.

According to the Lemma 1, we can figure out that the sliding surface defined in Eq.(17) will be driven onto the plane of $s = 0$ in finite time, which can be mathematically described as

$$T_r \leq \frac{1}{\lambda_1 \left(1 - \frac{\rho+1}{2} \right)} \ln \frac{\lambda_1 V_0^{\frac{\rho+1}{2}} + \lambda_2}{\lambda_2} \quad (36)$$

From Eq.(14) and Eq.(17), it can be seen that the plane $s = 0$ is not qualified to meet the condition of head pursuit intercept, which is $e = 0$. Therefore, we prove that the system can reach the origin from the sliding surface.

When $s \rightarrow 0$, if $\dot{e} > 0$, then $\beta |e|^\alpha \text{sign}(e) < 0$. As a result, $e < 0$ and the parameter e will increase along with the increase of time, and finally tends to zero. If $\dot{e} < 0$, then $\beta |e|^\alpha \text{sign}(e) > 0$, so $e > 0$, and

e will decrease until finally tends to 0 too. This shows that the states of the system will converge to the origin in finite time.

5 SIMULATION EXPERIMENT AND ANALYSIS

In this section, we apply the proposed approach in experimental scenario by using numerical simulation to validate the effectiveness.

Table 1: Simulation parameters setup.

Interceptor	Target	Guidance
$V_I = 1600m/s$	$V_T = 2000m/s$	$n = 2$
$\tau_I = 0.2s$	$\tau_T = 0.2s$	$\tau = 0.2s$

Notably, the targets with constant velocity and constant maneuvering (20g,-20g) are considered to test the designed method. Moreover, we analyze the change of interceptor trajectory, overload and sliding surface in multiple attack angles. The simulation parameters are given in Table 1.

According to Table 1, when the initial LOS angle q is 20 deg, the initial distance between the target and interceptor is $r(0) = 3000m$, $a_r = [-20, 0, 20]g$ and $\theta_r = 0$. 3 scenarios are tested: non-maneuvering target and two constant maneuvering targets. In Figure 3, the trajectories of both interceptor and target are graphically demonstrated.

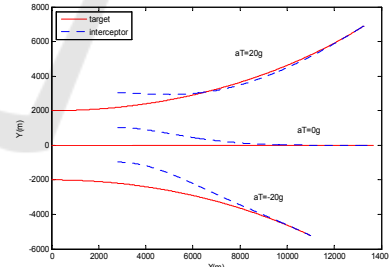


Figure 3: Response curves of intercept trajectory.

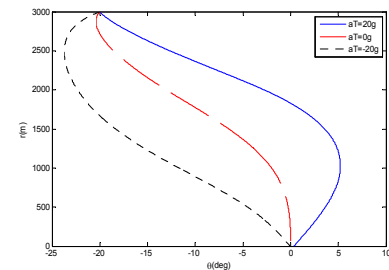


Figure 4: Response curves of trajectories in target coordinate system; $\theta_r = 0$ deg.

From Figure 3 we can see that, whether if the target has maneuvering or not, the trajectory of interceptor will gradually approach to the trajectory of target and track it until it is caught up. In Figure 4 and 5, the relative trajectories of interceptor in non-rotating polar coordinate attached to the target are given. It can be seen from the figure that, the interception is successfully achieved in the presence of target maneuvers and the initial heading errors ($\theta(0) = -20\text{deg}$), while the angle error is small. To be specific, as we set $\theta_r = 0$ in Figure 4, the angle errors are 0.34deg and 0.05deg while the a_r of target maneuvering are $20g$ and $-20g$, respectively. In Figure 5, θ_r is set to be -10deg .

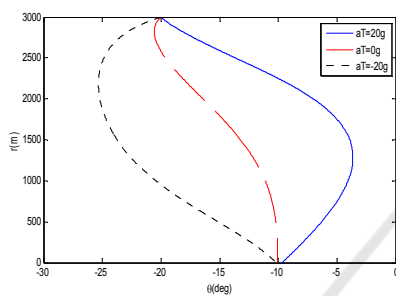


Figure 5: Response curves of trajectories in target coordinate system; $\theta_r = -10\text{deg}$.

From the experimental results we can see that, the angle errors are 0.12deg and 0.29deg separately, while the corresponding a_r of target maneuvering are $20g$ and $-20g$. Moreover, both Figure 4 and 5 show that the angle error is almost zero if the target has no maneuver.

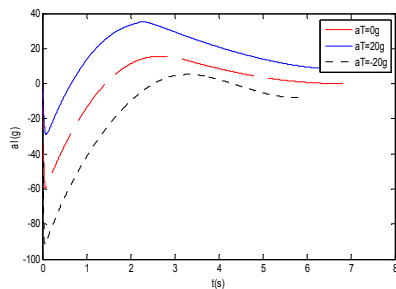


Figure 6: Response curves of interceptor acceleration; $\theta_r = 0\text{deg}$.

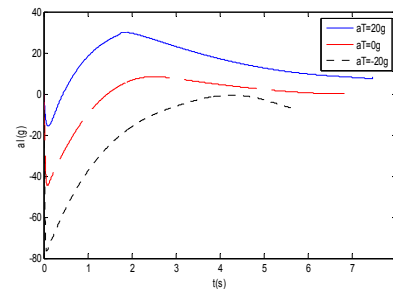


Figure 7: Response curves of interceptor acceleration $\theta_r = -10\text{deg}$.

Considering that both target and interceptor are set to be the typical high-speed target, the results show a good performance. As shown in Figure 6 and 7, the response curves of interceptor acceleration for different target maneuvers are presented respectively, where $\theta_r = 0$ and $\theta_r = -10\text{deg}$.

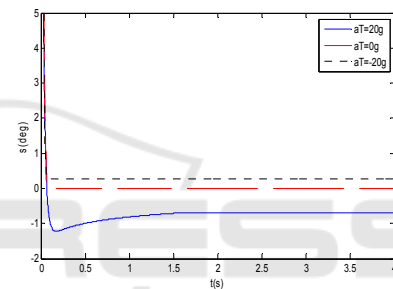


Figure 8: Response curves of sliding surface value; $\theta_r = 0\text{deg}$.

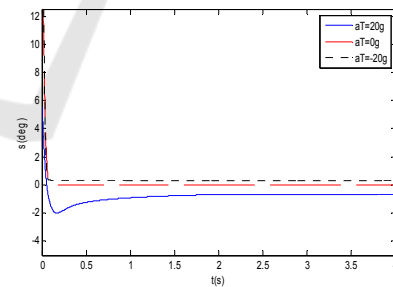


Figure 9: Response curves of sliding surface value; $\theta_r = -10\text{deg}$.

We can see that the magnitude of the interceptor acceleration is adjusted dynamically over time. The change of interceptor acceleration decreases after a short period of time. Finally, the tracking of target is realized. Compared with the head pursuit guidance laws that proposed in recent years, the maneuvering acceleration of interceptor is greatly reduced.

The value of the sliding variable for $\theta_r = 0$ and $\theta_r = -10\text{deg}$ are graphically showed in Figure 8 and 9, respectively. Obviously, it also can be seen from Figure 8 and 9 that, the sliding variable s could convergence to the sliding surface rapidly, then reach steady state.

In order to further illustrate the effectiveness and the advance of the guidance law, we compared it with the guidance law proposed in paper (Dan, 2013). Table 2 shows the intercept time under different target maneuvers.

Moreover, in order to evaluate the convergence rate of the proposed method, the comparison of interception time between our method and the guidance law proposed in (Dan, 2013) are presented. The comparison results are given in the Table 2, in which 4 target acceleration values are applied.

Table 2: Intercept time of the two guidance law.

a_T	10g	15g	20g	25g
Our	8.413s	7.982s	7.523s	7.051 s
Dan	13.827s	13.304s	12.506s	11.563s

We can see that the guidance law proposed in this paper has shorter intercept time and has better convergence performance.

6 CONCLUSIONS

In this paper, a finite time convergent guidance law for head pursuit is proposed, in which the terminal sliding mode control theory is used. By considering the dynamics characteristics of target and interceptor, an adaptive law is theoretically designed based on the interference factors of target maneuvering and model errors. The results of numerical simulation show that the guidance law can be implemented on the head pursuit intercept of high-speed targets and achieve successful interception in different attack angles and target maneuvering, while having smaller intercept error compared with other methods. The proposed method has lower requirement on the way of maneuvering, which show a potential application in real interception of high-speed vehicle. Moreover, the sliding variable can also convergence to sliding surface more quickly with strong robustness.

ACKNOWLEDGEMENTS

This work was supported by the National Natural Science Foundation of China under Grant 61502391,

the Foundation of National Key Laboratory of Aerospace Flight Dynamics and the China Space Foundation under Grant 2015KC020121.

REFERENCES

- Shima, T., & Golan, O. M. (2007). Head pursuit guidance. *Journal of Guidance, Control, and Dynamics*, 30(5), 1437-1444.
- Goyal, V., Deolia, V. K., & Sharma, T. N. (2015). Robust Sliding Mode Control for Nonlinear Discrete-Time Delayed Systems Based on Neural Network. *Intelligent Control and Automation*, 6(01), 75.
- Zhihong, M., Paplinski, A. P., & Wu, H. R. (1994). A robust MIMO terminal sliding mode control scheme for rigid robotic manipulators. *Automatic Control, IEEE Transactions on*, 39(12), 2464-2469.
- Feng, Y., Yu, X., & Han, F. (2013). High-order terminal sliding-mode observer for parameter estimation of a permanent-magnet synchronous motor. *Industrial Electronics, IEEE Transactions on*, 60(10), 4272-4280.
- Kumar, S. R., Rao, S., & Ghose, D. (2014). Nonsingular terminal sliding mode guidance with impact angle constraints. *Journal of Guidance, Control, and Dynamics*, 37(4), 1114-1130.
- Liu, Y. J., & Li, Y. X. (2010). Adaptive fuzzy output-feedback control of uncertain SISO nonlinear systems. *Nonlinear Dynamics*, 61(4), 749-761.
- Li, P., & Yang, G. (2011). An adaptive fuzzy design for fault-tolerant control of MIMO nonlinear uncertain systems. *Journal of Control Theory and Applications*, 9(2), 244-250.
- Gu, Y. J., Yin, X. X., Liu, H. W., Li, W., & Lin, Y. G. (2015). Fuzzy terminal sliding mode control for extracting maximum marine current energy. *Energy*, 90, 258-265.
- Zhao, D., Zhu, Q., & Dubbeldam, J. (2015). Terminal sliding mode control for continuous stirred tank reactor. *Chemical Engineering Research and Design*, 94, 266-274.
- Behera, A. K., & Bandyopadhyay, B. (2015). Steady-state behaviour of discretized terminal sliding mode. *Automatica*, 54, 176-181.
- Madani, T., Daachi, B., & Djouani, K. (2015). Non-singular terminal sliding mode controller: Application to an actuated exoskeleton. *Mechatronics*, 33, 136-145.
- Lu, K., Xia, Y., Zhu, Z., & Basin, M. V. (2012). Sliding mode attitude tracking of rigid spacecraft with disturbances. *Journal of the Franklin Institute*, 349(2), 413-440.
- Lee, D., & Vukovich, G. (2015). Adaptive sliding mode control for spacecraft body-fixed hovering in the proximity of an asteroid. *Aerospace Science and Technology*, 46, 471-483.
- Hua, W., & Chen, X. (2011). Adaptive sliding-mode guidance law for head pursuit. *Journal of Harbin Institute of Technology*, 43(11), 30-33.

- Song, J., & Song, S. (2015). Three-dimensional guidance law based on adaptive integral sliding mode control. *Chinese Journal of Aeronautics*, 29(1), 202-214.
- Yu, S., Yu, X., Shirinzadeh, B., & Man, Z. (2005). Continuous finite-time control for robotic manipulators with terminal sliding mode. *Automatica*, 41(11), 1957-1964.
- Dan Yang. (2013). Research on variable structure terminal guidance law of space interception. *Shanghai Jiao Tong University*.

